Schwann Cell and Axon Electrical Potential Differences

Squid nerve structure and excitable membrane location

RAIMUNDO VILLEGAS, LEOPOLDO VILLEGAS, MÁXIMO GIMÉNEZ, and GLORIA M. VILLEGAS

From the Departamento de Biofísica, Instituto Venezolano de Investigaciones Científicas (I.V.I.C.), Caracas, Venezuela

ABSTRACT In fifty-seven resting nerve fibers of the squid *Sepioteuthis sepioidea* impaled from outside to inside, three potential difference (PD) levels were recorded. In twelve nerve fibers the position of the tip of the micropipette, when it was recording one of the PD levels, was labeled with carmine, and the minute spot of dye was localized histologically. The first PD level of −10 to −26 mv, was located in the endoneurium cells; the second level, formed by a single PD of −33 to −46 mv, was located in the Schwann cell; and the third level, formed by a single PD of −50 to −65 mv, was located in the axon. In sixteen nerve fibers the independence among these PD levels was demonstrated as follows. One micropipette was inserted inside the axon for recording its PD; a second one was inserted inside one endoneurium cell or inside one Schwann cell for recording the PD; and a third micropipette was inserted inside the axon to supply current to depolarize the axon. When the axon was depolarized no significant change was observed in the PD of either the endoneurium cell or the Schwann cell. In all nerve fibers action potentials were registered from the axon only. This identifies the axolemma (axon plasma membrane) as the excitable membrane.

INTRODUCTION

Physiologists have traditionally assumed that the electrical potential differences which characterize the nerve fiber during rest and during the propagation of an impulse occur across a surface membrane of the nerve fiber. The identification of the structure corresponding to the excitable membrane of a nerve fiber has been a challenging problem in neurobiology. Schmitt (1, 2), has suggested that the excitable membrane may be a composite of the axolemma (plasma membrane of the axon proper) and the Schwann

cells, and Sjöstrand (3) has proposed that the excitable membrane may be formed by a fusion of the axolemma and the inner Schwann cell plasma membrane. Frankenhaeuser and Hodgkin (4) have suggested the existence of a space separating the axon surface from the periaxonal layers.

Our previous studies of the ultrastructure of the squid *Doryteuthis plei* giant nerve fiber (5, 6), and of its permeability to water and small non-electrolyte molecules (6–8) indicated the axolemma alone as the excitable membrane. It was found (*a*) that the Schwann layer is crossed by slit channels about 60 A wide, though the membrane of individual Schwann cells is continuous; (*b*) that the axolemma and the inner Schwann cell membrane are separated by a space approximately 80 A wide, which can be narrowed and broadened by osmotically induced volume changes of the limiting cells; and (*c*) that the resting axolemma is crossed by pores of 4.0 to 4.5 A in radius. These results suggested that the axolemma is the only barrier between the axoplasm and the nerve outside which is capable of maintaining the ionic concentration differences necessary for normal nerve function. See references 6 to 8 for further discussion.

To decide among these alternative suggestions (1–3, 6–8) as to the identification of the excitable membrane one must record simultaneously from a Schwann cell and from the axon during the passage of an action potential. As Schmitt (2) has pointed out, the difficulty arises in finding a nerve in which micropipettes can be inserted simultaneously in a Schwann cell and in the axon. Fortunately, the giant nerve fiber of the squid *Sepioteuthis sepioidea*, found in Venezuelan coastal waters, possesses Schwann cells which permitted this investigation.

The present work deals with: (I) the ultrastructure of the *S. sepioidea* giant nerve fiber; (II) its electrical potential profile; (III) the location of the various levels of electrical potential differences; and (IV) the electrical independence of the Schwann cell potential from that of the axon. The results herein reported identify the axolemma as the excitable membrane and show the electrical independence of the potentials observed in the Schwann cell and in the axon.

Part of this work has been published as a preliminary note (9).

I. NERVE FIBER STRUCTURE

Experimental Method

The giant nerve fibers from the first paramedial stellar nerves of *S. sepioidea* were isolated from the animals in less than 10 minutes, and fixed in 2 per cent osmium tetroxide or 0.6 per cent potassium permanganate according to a previously described technique (5). Araldite was used as embedding medium. Fine sections obtained in a LKB ultramicrotome were examined in a Siemens Elmiskop I.

Results and Discussion

As shown in Fig. 1, the structural pattern of the giant nerve fibers of *S. sepioidea*, which are 250 to 450 μ in diameter, is similar to that found in *D. plei*.

In *S. sepioidea* the axolemma, about 80 A thick, is separated from the inner Schwann cell surface by a space 40 to 120 A wide. The Schwann layer is 1.5 to 5 μ thick and is formed by a single row of Schwann cells. The thickness of this layer is about ten times that of *D. plei* and *Loligo pealii* (10). At their outer surfaces, the Schwann cells are covered by a basement membrane approximately 0.2 μ thick which follows the numerous invaginations of the cell surface. These invaginations of the Schwann cell surface are deeper than those in *D. plei* (5–6) or in *L. pealii* (10). The lateral surfaces of the Schwann cells are irregular also and the neighboring cells imbricate along their apposed surfaces. Thus, the intercellular limits are tortuous pathways which account for some of the continuous channels crossing the Schwann cell layer. As in *D. plei* (6), other channels are formed by the close apposition of two or more finger-like processes of a single Schwann cell. Fig. 2 shows the system of paired osmiophilic lines which form the Schwann cell channels. As shown in Fig. 3, the axolemma and the Schwann cell membrane, including the channel walls, are formed by a three layered unit membrane approximately 80 A thick. The channel width varies from 40 to 120 A.

The endoneurium, of which about a 20 μ thick layer is left after dissection of the fiber, is formed by alternating layers of connective tissue fibrils and cells and lies outside the basement membrane. The limit between the endoneurium and the basement membrane is rather equivocal as shown in Figs. 1 and 2. The endoneurium cells and connective tissue fibrils (which are less than 500 A thick) are embedded in an amorphous material similar to the basement membrane. The endoneurium cell bodies in cross-section are about 1 to 6 μ thick and extend for several micra alongside the nerve. They flatten down towards their edges. A cross-section of a fiber shows not less than twenty endoneurium cells.

The dimensions given were obtained from nerve fibers fixed and embedded as described above. A certain amount of shrinkage is to be expected. Therefore, the true dimensions in the unfixed fibers should be larger.

II. ELECTRICAL POTENTIAL PROFILE OF THE SQUID NERVE FIBER

Experimental Method

Electrical potential differences were measured in fifty-seven resting nerve fibers at 22–24°C, in a Faraday screening cage. Each isolated nerve fiber, as shown in Fig. 4, was placed within a lucite chamber containing artificial sea water, with the following

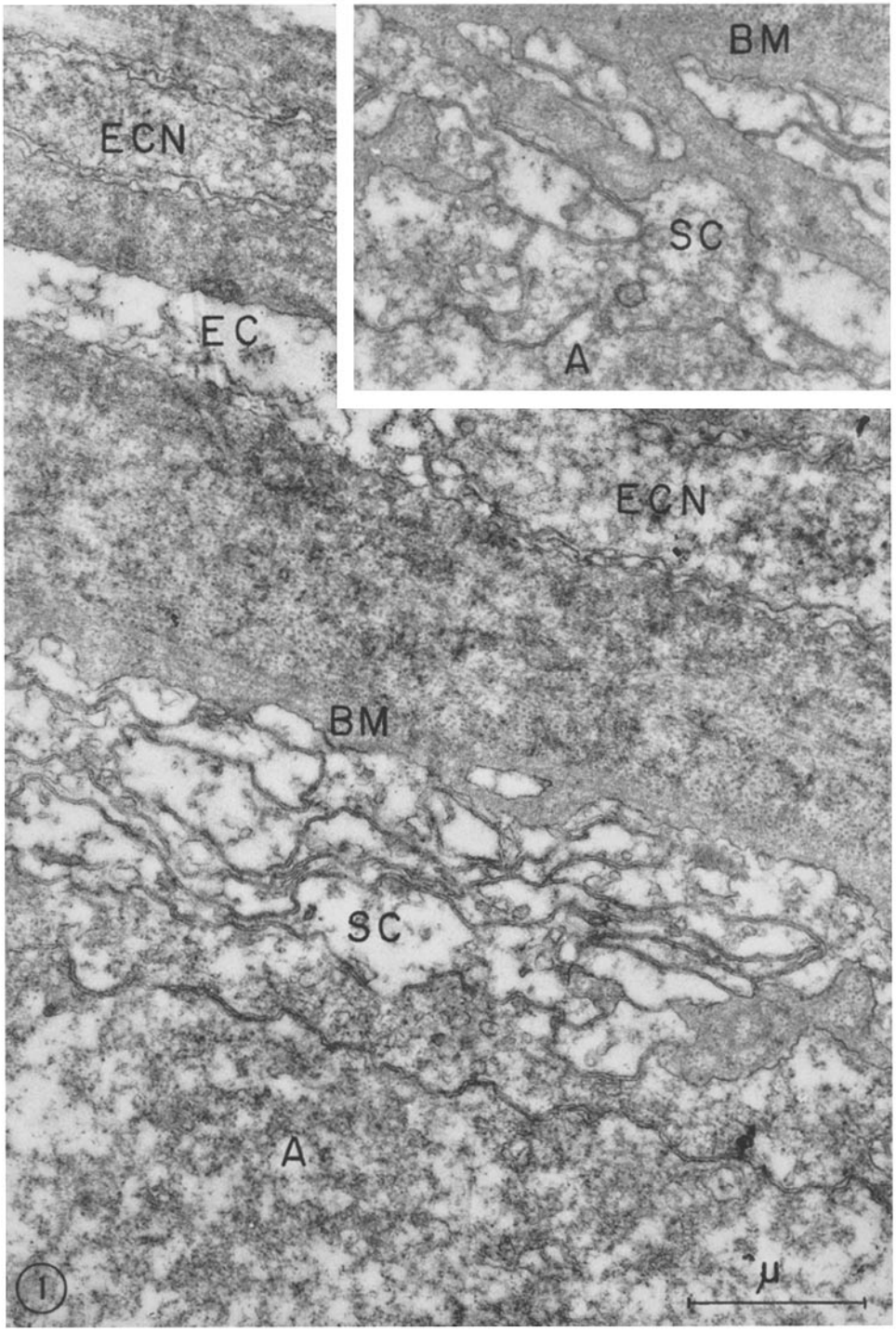
ECN
EC
BM
SC
A
ECN
BM
SC
A
1
μ

composition, in millimols per liter: NaCl, 441.7; KCl, 9.9; $CaCl_2$, 11.0; $MgCl_2$,53.1; $NaHCO_3$, 2.5 (reference 11). The nerve fiber in the chamber was kept under slight tension by means of threads tied at each end.

Electrical potential differences were measured by means of glass micropipettes. The micropipettes, with tips smaller than 0.5 μ (12), were prepared with an Alexander and Nastuk micropipette puller (13) from pyrex tubes with an internal diameter of about 1 mm and an external diameter of about 2 mm. Micropipettes were filled with 3 M KCl solution by boiling under reduced pressure. The exploring micropipette was connected to a calomel electrode by means of a KCl-agar bridge. A symmetrical calomel electrode used as indifferent electrode was connected *via* a KCl-agar bridge to a flask filled with 20 ml of sea water; the flask was connected to the sea water bath *via* a sea water–agar bridge. Both electrodes were connected to a high impedance voltmeter (Keithley 200 B, 10^{14} ohms input impedance, grid current less than 5×10^{-14} amperes) whose output was fed into a recorder (Sefram TS3VA and PHD7). The micropipette resistance and tip potential were measured in artificial sea water before and after each penetration. The criteria for acceptable micropipettes were: suitable shape, tip resistance between 5 and 15 megohms, and tip potential between 0 and −5 mv. The circuit used to measure the intracellular potentials in the resting nerve is shown in Fig. 4.

The exploring micropipette was advanced with a micromanipulator into the fiber along a line perpendicular to its surface under a stereoscopic microscope at a magnification of 72 or 216×.

Results and Discussion

As shown in Fig. 5, when the micropipette was moved from outside the resting nerve fiber through the endoneurium, the Schwann cell layer, finally reaching the axon inside, three potential difference levels relative to the sea water bath, were recorded: (*a*) the first level is formed by one or more potential differences of −10 to −26 mv; (*b*) the second level is a single potential difference of −33 to −46 mv; and (*c*) the third level is a single potential difference of −50 to −65 mv. Values obtained in ten successive penetrations in nerve fibers 10 and 50 are shown in Table I. The mean ± standard errors for the three potential difference levels in the last six nerve fibers utilized are shown in Table II.

(*a*) The potential differences that comprised the first level were observed in all penetrations that reached the axon. Since these potential differences were found immediately after penetrating the nerve fiber from outside they were considered to correspond to the endoneurium cells. A cross-section of a nerve fiber shows no less than twenty endoneurium cells surrounding the axon. In

FIGURE 1. Electron micrograph of a giant fiber cross-section showing axon (*A*), Schwann cell (*SC*), basement membrane (*BM*), and two endoneurium cells (*EC*) with their nuclei (*ECN*). Insert shows the continuation to the right of the Schwann layer. Note the deep invaginations of the basement membrane into the Schwann cell. Nerve fixed in OsO_4.

some of the penetrations (Fig. 5 *c*) as the exploring micropipette was advanced, the potential difference was observed to fall one or several times to ground potential before reaching the second potential level. This suggests that the micropipette has passed through the large intercellular spaces that separate the endoneurium cells. In the cases in which these falls to ground potential

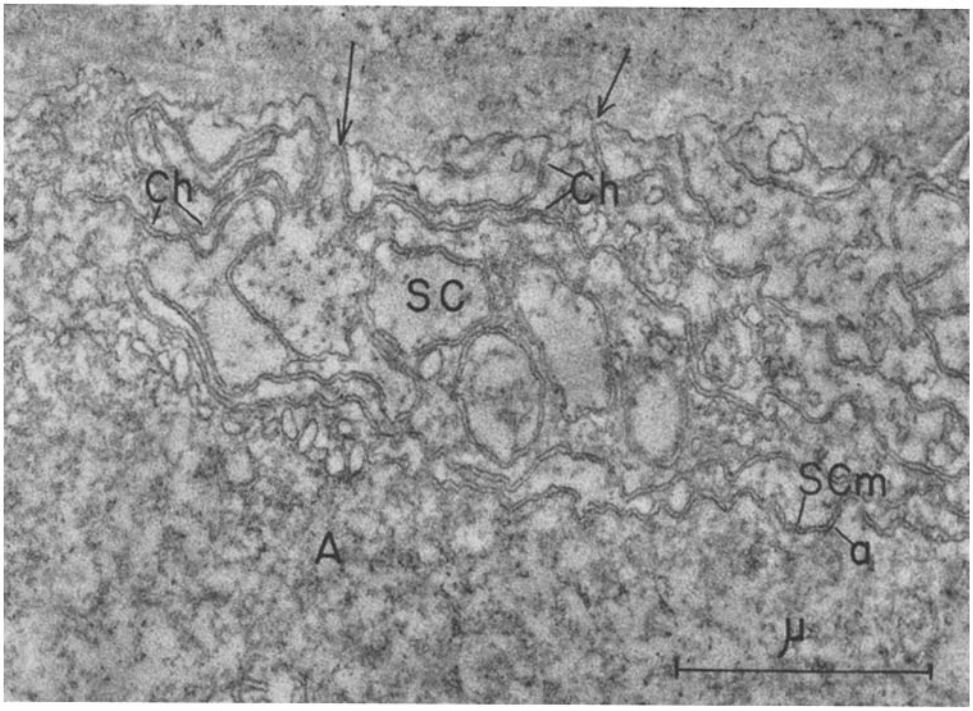

FIGURE 2. Electron micrograph showing the axon (*A*) and the Schwann cell layer (*SC*). The space between the axolemma (*a*) and the Schwann cell plasma membrane (*SCm*) is observed. The Schwann cell layer is crossed by channels (*Ch*). The double osmiophilic lines forming the channel walls are continuous with the Schwann cell plasma membrane as indicated by arrows. Nerve fixed in OsO_4.

were not observed (Figs. 5 *a* and 5 *b*) it may be assumed that the micropipette pushed the cells together and obliterated the intercellular spaces.

(*b*) The single potential difference that formed the second level was measured in all the nerve fibers, but not necessarily in all the penetrations in a single fiber. In the first two nerve fibers that were examined this second level was measured in only one out of ten trials. The proportion increased to six out of ten trials in the last two nerves; this may be due to better technique gained from experience. The fact that it was not possible to measure the second level in all individual penetrations in a single nerve fiber suggested that this potential level was related to a cellular type forming a thin and single layer. This po-

tential difference level could sometimes be recorded over periods up to 10 minutes, its stability indicating effective sealing around the micropipette tip and little cellular damage. At this stage of the investigation the second level was tentatively considered to correspond to the Schwann cell layer electrical potential.

In some nerves the micropipette was made to cross the axon, in order to ex-

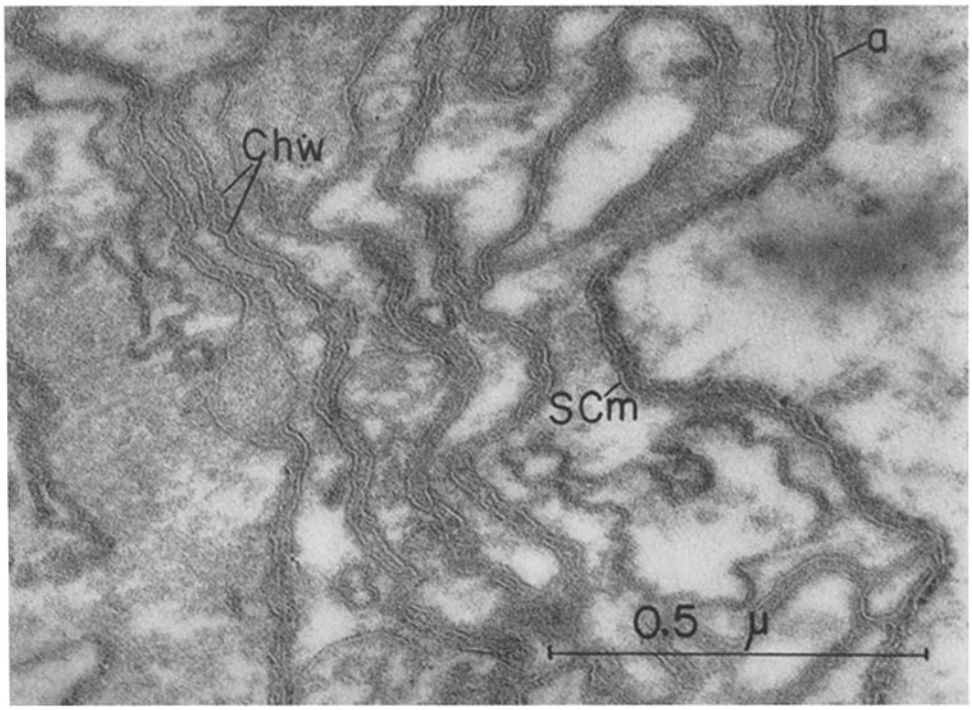

FIGURE 3. Electron micrograph showing the unit membrane structure of the Schwann cell plasma membrane (*SCm*), the channel walls (*Chw*), and the axolemma (*a*). The width of the channel and the axon-Schwann cell space varies from 40 to 120 A. Nerve fixed in $KMnO_4$.

plore the nerve surface from the inside towards the outside. As shown in Fig. 6, immediately after the micropipette is moved from the axoplasm towards the outside, a rise from the axon resting potential to the second potential level is registered. This was observed in nine out of ten trials. When the micropipette was moved backwards to the axoplasm, the axon resting potential was again recorded. These observations are in accord with the identification of this potential level with the Schwann cell layer.

(*c*) The third level ranging from -50 to -65 mv corresponds to the well known resting potential of the axon. When the micropipette was moved inside the axoplasm no change in this potential was observed.

III. LOCATION OF THE ELECTRICAL POTENTIAL DIFFERENCES IN THE RESTING NERVE FIBER

Experimental Method

To corroborate the location ascribed to the potential difference levels described in section II, the recording sites were marked by Villegas' (14) modification of Mitarai's technique (15). The technique is based on the histological localization of a minute carmine spot deposited in the tissue by electrophoresis from the tip of the exploring

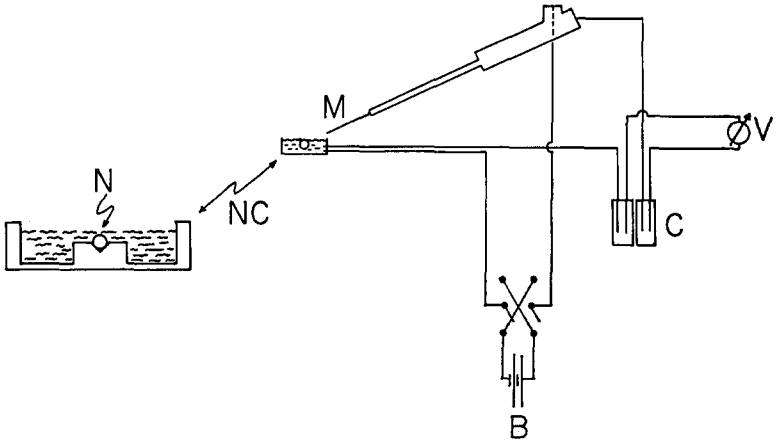

FIGURE 4. Circuit used to measure the intracellular potential differences in the resting nerve. Details are described in section II. *M* = micropipette, *C* = calomel electrodes, and *V* = high impedance voltmeter. The circuit utilized to label the site of potential difference measurement is also shown. Details are described in section III. For labeling, carmine lithium was transferred from the tip of the micropipette to the tissue by electrophoresis, using current from battery *B*, whose polarity could be reversed by means of the double-pole double-throw switch. A cross-section of the lucite nerve chamber (*NC*), with a nerve fiber (*N*), is also shown.

micropipette. Besides the circuit used for potential difference measurements, another circuit in parallel, different from that employed for the potential measurements, was used for the electrophoresis. This allowed the measurement of the potential difference before and after marking, without moving the micropipette, thus giving considerable certainty to the location (14).

Micropipettes were filled with a 3 M KCl–carmine lithium solution. They were prepared by removing from micropipettes previously filled with 3 M KCl, most of the 3 M KCl solution, except that within the tip, and replacing it by a carmine lithium solution in 3 M KCl. The carmine solution was prepared by adding 1.2 gm of carmine lithium (Matheson, Coleman, and Bell) to 10 ml of 3 M KCl solution adjusted to pH 9. Since alkalinity increases carmine solubility, the 3 M KCl used to fill the micropipettes was adjusted to pH 9 by addition of KOH. The micropipette was connected exactly

as described in section II. The criteria for acceptable micropipettes were the same.

The circuit used for the electrophoresis is shown in Fig. 4. One copper wire was placed in the KCl bridge of the exploring micropipette and another one in a sea water–agar bridge immersed in the sea water bathing the nerve. Both wires were connected

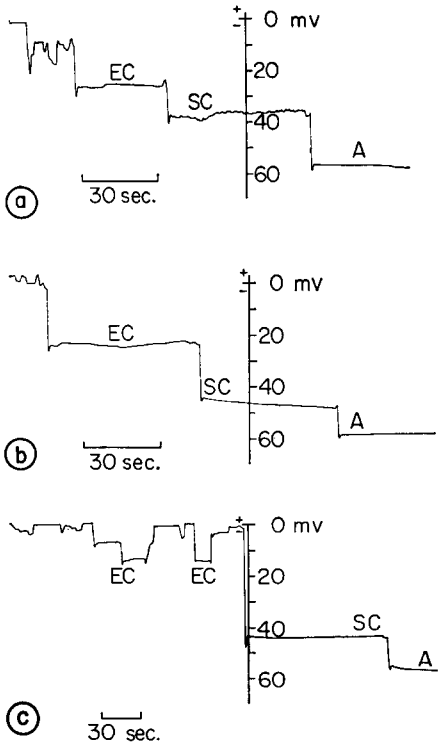

FIGURE 5. Records of the electrical potential profile of the squid nerve fiber. When the micropipette was moved from outside the nerve towards the inside three potential difference levels were found. The first level is formed by one or several potential differences corresponding to the endoneurium cells (*EC*), the second and third levels are formed by single potential differences corresponding to the Schwann cell (*SC*) and axon (*A*), respectively. When it was possible the micropipette was stopped and the potential differences observed. (*a*) Corresponds to a penetration in nerve 7, axon diameter 290 μ; (*b*) corresponds to a penetration in nerve 10, axon diameter 310 μ; (*c*) corresponds to a penetration in nerve 17, axon diameter 410 μ. See section II for further explanation.

via a double-pole double-throw switch to a 100 volt battery. This circuit, without passing the current through the calomel electrodes, permits positive and negative voltages to be applied to the exploring micropipette in order to move the carmine out of the micropipette. Voltages were applied to the micropipette, only during a fraction of a second, the time necessary to pass the lever of the switch back and forth between the contacts.

After recording a potential difference corresponding either to the first, the second, or the third level with the technique described in section II, a positive voltage was

TABLE I

POTENTIAL DIFFERENCE LEVELS*
RECORDED IN TEN SUCCESSIVE PENETRATIONS
IN TWO SQUID NERVE FIBERS

Penetration	First level	Second level	Third level
	Nerve 10; axon diameter 290 μ; temperature 24°C		
	$-mv$	$-mv$	$-mv$
1	11; 15	—	58
2	26	—	59
3	14	—	58
4	11; 24	38	60
5	18	—	59
6	15; 22	36	59
7	13	—	60
8	15; 23	45	60
9	15	40	60
10	16	42	59
	Nerve 50; axon diameter 360 μ; temperature 23°C		
1	24; 26	42	60
2	10; 18	—	60
3	24; 20; 18	44	60
4	18; 24	36	62
5	10	—	60
6	18; 14; 24	46	60
7	24; 14; 16	36	60
8	18	—	60
9	22	38	60
10	16	44	60

* Referred to the sea water bath.

TABLE II

POTENTIAL DIFFERENCE LEVELS* IN SIX SQUID NERVE FIBERS

Nerve No.	No. of impalements	Endoneurium cells	Schwann cells	Axon
		$-mv$	$-mv$	$-mv$
52	19	17 ± 0.9 (36)	39 ± 0.3 (10)	56 ± 0.1
53	23	20 ± 0.6 (44)	39 ± 0.9 (11)	60 ± 0.1
54	19	20 ± 0.9 (39)	42 ± 1.1 (12)	60 ± 0.1
55	21	19 ± 0.8 (46)	39 ± 1.1 (10)	52 ± 0.3
56	14	18 ± 1.1 (16)	36 ± 1.3 (8)	54 ± 0.3
57	17	18 ± 1.1 (46)	41 ± 1.0 (10)	60 ± 0.1

Numbers in parentheses are numbers of endoneurium cells and Schwann cells impaled.
* Referred to the sea water bath. Values are the mean ± standard error of the mean.

applied to the micropipette and then the polarity was reversed. In this manner a minute amount of carmine was transferred to the tissue. The potential difference was measured again without moving the micropipette tip, thus giving considerable certainty to the location. A single carmine deposition was made in each nerve.

Immediately after the measurements were concluded, the micropipette was withdrawn and the nerve fixed in Bouin's solution and embedded in paraffin. About 400 sections were made, each approximately 5 μ thick, and the carmine spot was searched for with a phase contrast microscope at a magnification of 560 ×. After location of the carmine spot, the sections were counterstained with hematoxylin-eosin to relate the position of the spot to the cell nuclei.

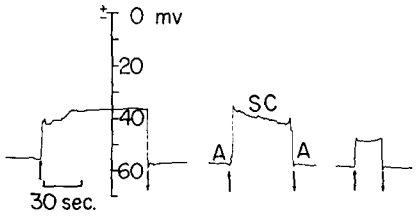

FIGURE 6. Rise in the potential difference tracing observed when the tip of the exploring micropipette is passed through the axon, to impale a Schwann cell at the opposite nerve wall. When the tip of the micropipette is moved into the axoplasm, a drop from the Schwann cell potential difference (*SC*) to the axon potential difference (*A*) is recorded. The potential differences of three Schwann cells in the same nerve are presented. Nerve 34, axon diameter 450 μ.

Results and Discussion

In twelve isolated nerve fibers, the three potential levels described in section II were measured and the site, corresponding to one of the levels, was labeled with carmine.[1]

In two nerve fibers, on which sites corresponding to the first level were labeled, the carmine spots were located in the endoneurium; the labeled endoneurium cells of these nerves had potential differences of −24 and −22 mv, respectively.

In eight nerve fibers, single sites corresponding to the second potential level were labeled. The carmine spots corresponding to seven nerve fibers were located in Schwann cells with potential differences of −35, −39, −33, −43, −37, −40, and −41 mv, respectively. In one nerve fiber the carmine spot could not be found in the histological sections. Fig. 7 shows the carmine spot in a Schwann cell with a potential difference of −41 mv, corresponding to nerve fiber 32. The carmine spot is clearly seen within a Schwann cell and

[1] No difference was observed between measurements made with micropipettes containing 3 M KCl or 3 M KCl–carmine lithium. This has already been noted in other tissues by Villegas (14) and by Whittembury (16).

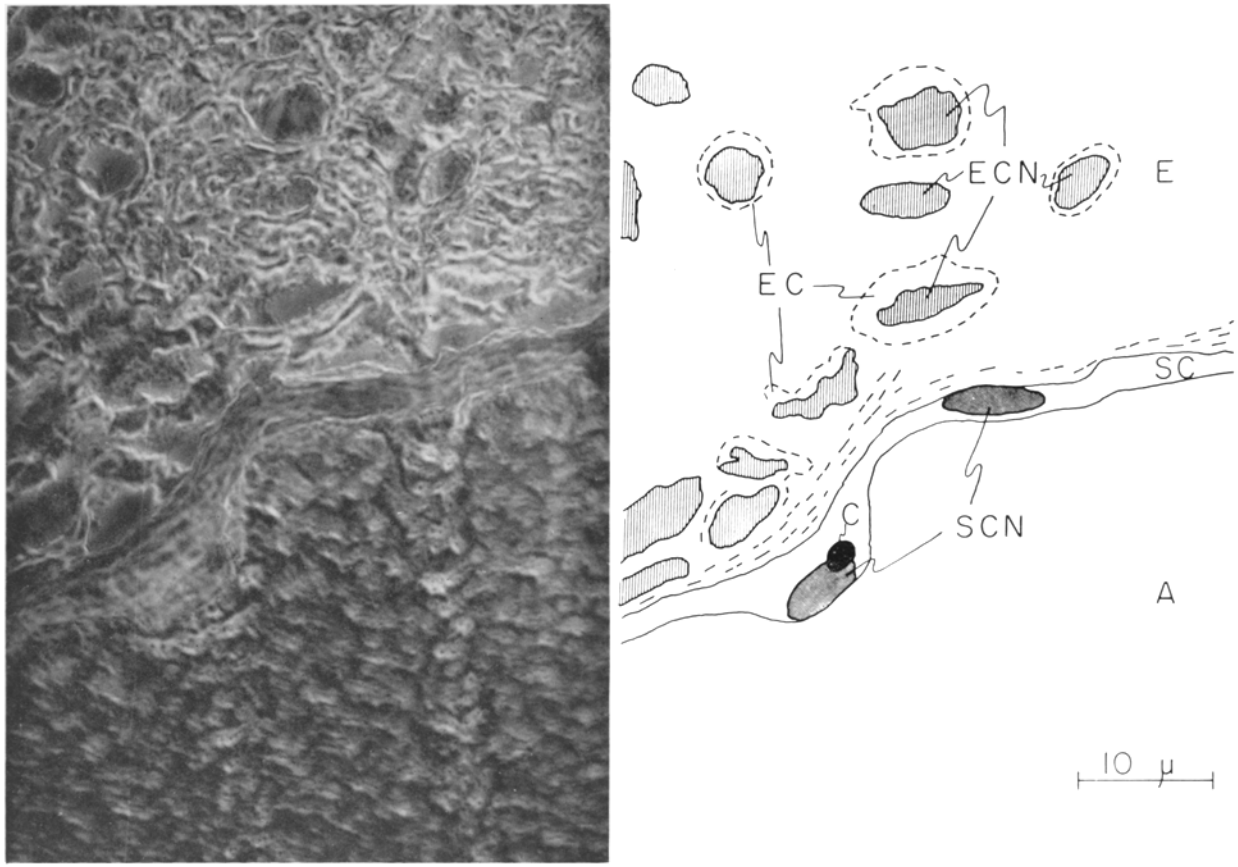

FIGURE 7. Location of the Schwann cell electrical potential difference. At the left side appears a phase contrast micrograph of a stained, 5 μ thick, cross-section of nerve fiber 32. The drawing at the right represents a schema of the micrograph showing the situation of the axon (*A*), the Schwann cells (*SC*), and the endoneurium (*E*). Several endoneurium cells (*EC*) and their nuclei (*ECN*) are shown. Two Schwann cell nuclei (*SCN*) are observed. The carmine spot (*C*) is located on the Schwann cell nucleus at the left, which appears pale and blurred for its situation out of the focal plane. The increase in the Schwann cell thickness at the site of the carmine spot may be due to the microelectrode impalement. This carmine spot was located in a Schwann cell with a -41 mv potential difference.

close to its nucleus. The potential differences recorded after labeling were never lower than 8 mv from the value recorded before labeling. This difference may be due partly to small changes in the electrode tip potential that were observed after voltage was applied during marking, and partly to the small amount of ions injected into the cell. The agreement between the potential differences recorded before and after the carmine was injected suggests that no rupture of the cell membrane occurred during labeling.

In two nerve fibers, sites corresponding to the third level, with potential differences of -50 and -60 mv respectively were labeled, and the carmine spots were located inside the axon.

The results presented here indicate the endoneurium cells as the origin of the first level of potential difference, the Schwann cell as the origin of the second level, and the third level as the resting potential of the axon. These results agree with the conclusions of the previous section.

IV. ELECTRICAL INDEPENDENCE OF THE ENDONEURIUM CELLS AND THE SCHWANN CELLS FROM THE AXON

Experimental Method

In order to identify the spike-generating cell, and to investigate the relationships between the potential differences of the endoneurium cells, the Schwann cells, and the axon, the following experiments were made. With three micromanipulators three micropipettes, similar to those described in section II, were simultaneously inserted along the nerve, the tips being 100 to 150 μ apart. The first, M′, was inserted inside the axon to record its potential. The second, M″, was inserted inside one endoneurium cell or one Schwann cell for potential recording. The third micropipette, M‴, was inserted inside the axon and was used to supply current from a battery to depress the potential of the axon. The total distance between the first and the third micropipettes was never greater than one axon diameter. The exploring micropipettes were provided with Ag-AgCl electrodes in the 3 M KCl and were connected to cathode followers (Grass MEP 6). The cathode followers were fed into a dual beam oscilloscope (Tektronix 551; plug in units D) *via* DC amplifiers (Grass P6B). The oscilloscope tracings were recorded either with a movie camera (Grass C4G) or a photographic camera (Tektronix C12). The intracellular potentials were referred to another Ag-AgCl electrode immersed in 3 M KCl connected to the earthed sea water bathing the nerve *via* a sea water–agar bridge.

As shown in Fig. 8, the micropipette that was used to depolarize the axon was connected to the sea water bath through a variable resistor, used as a voltage divider, and a 22.5 volt battery. The circuit could be switched on and off at will. With this experimental design, if the potential of the axon recorded by M′ is diminished by the current supplied through M‴, the potential difference at the axon region under M″ should be below or, at most, of the same value as that recorded by M′.

To obtain action potentials the nerve was stimulated using two external fine plati-

num wires connected *via* a stimulus isolation unit (Grass SIU-4B) to a stimulator (Grass S4E).

Results and Discussion

Fig. 9 shows records obtained from an axon and one endoneurium cell. In (*a*) the axon tracing shows a −56 mv resting potential and an action potential of

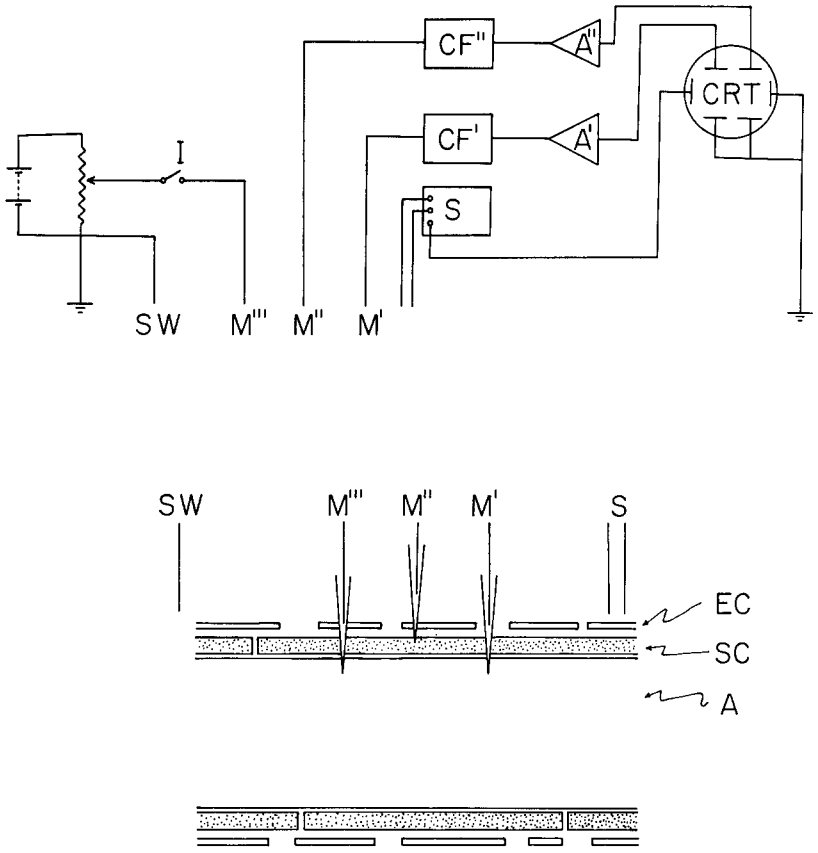

FIGURE 8. Circuit utilized to measure simultaneously the potential differences of the axon and the endoneurium cell or the Schwann cell. Details are described in section IV. *M'* = micropipette for recording the axon potential; *M''* = micropipette for recording the endoneurium cell or the Schwann cell potential; *CF'* and *CF''* = cathode followers; *A'* and *A''* = DC amplifiers; *CRT* = double beam cathode ray oscilloscope; *S* = stimulator. To the left is shown the circuit utilized to depolarize the axon. *M'''* = micropipette utilized to supply current inside the axon through a variable resistor acting as a voltage divider, from a 22.5 v battery. The interrupter, *I*, permits switching this circuit on and off. The reference electrode is connected *via* a sea water-agar bridge (*SW*) to the sea water bath. At the bottom may be seen a schematic drawing of a longitudinal section of the squid nerve fiber showing the electrodes in place and from outside towards inside, the endoneurium cells (*EC*), the Schwann cells (*SC*), and the axon (*A*).

96 mv, which is followed by an undershoot of 12 mv. The endoneurium cell tracing shows a resting potential of −22 mv and the absence of a rapid response during nerve impulse propagation. In (*b*) when the resting and action potentials of the axon are locally reduced below the endoneurium cell poten-

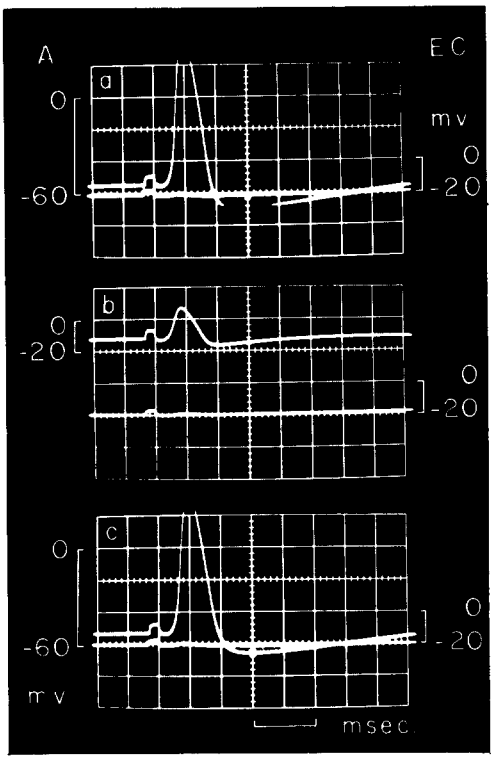

FIGURE 9. Simultaneous recordings from inside an axon (upper tracing; left scale), and from an endoneurium cell (lower tracing; right scale) with micropipettes *M'* and *M''* of Fig. 8. (*a*) Resting and action potentials typical of nerve were registered only from the axon. (*b*) The potentials of the axon reduced by current supplied from micropipette *M'''*. (*c*) Interruption of the current was followed by recovery of the resting and action potentials of the axon. Nerve 40; axon diameter 350 μ.

tial by means of externally supplied current, almost no change of the endoneurium cell potential is observed. The potential change of the endoneurium cell was always smaller than 3 mv. Since no significant change is produced by the supply of current, and since a change would be expected were the potential related to the axon potential, it follows that the −22 mv potential difference is being recorded from within an endoneurium cell. In (*c*) recovery of the potentials of the axon follows interruption of the external current supply. Similar results were obtained from sixteen nerve fibers, at temperatures ranging from 22–24°C.

In Fig. 10 are shown simultaneous tracings obtained from an axon and one Schwann cell in a nerve at rest and during impulse propagation. In (*a*) the axon tracing shows the typical resting and action potentials; the Schwann cell resting potential is −40 mv, and there is no spike during impulse conduction. In (*b*) are shown the potentials of the axon locally reduced by the externally

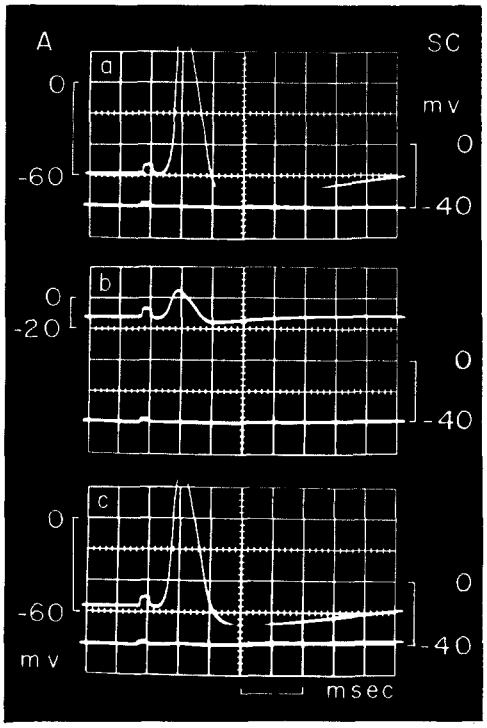

FIGURE 10. Simultaneous recording of the axon potential (upper tracing; left scale), and of the Schwann cell potential (lower tracing; right scale) with micropipettes *M'* and *M''* of Fig. 8. (*a*) Resting and action potentials typical of nerve were recorded only from the axon. (*b*) The axon potentials reduced by current supplied from micropipette *M'''*. (*c*) Interruption of the current was followed by recovery of the resting and action potentials of the axon. Nerve 40.

supplied depolarizing current, and almost no change of the Schwann cell potential is observed. The potential change of the Schwann cell was always smaller than 3 mv. Since no significant change is produced by the supply of current, and since a change would be expected were the potential related to the axon potential, it follows that the −40 mv potential difference is being recorded from within a Schwann cell. As shown in (*c*), recovery of the axon potentials follows interruption of the external current supply. Similar results were obtained from sixteen nerve fibers at temperatures ranging from 22–24°C.

The following comments, which do not affect our conclusions, are pertinent.

The small change sometimes observed in the endoneurium cell and Schwann cell potentials, during the passage of the current used to depolarize the axon, may be related either to the current flowing through the electrical resistances represented by the periaxonal layers, or to an artifact. The action potentials observed for the axons in Figs. 9 *b* and 10 *b*, may be ascribed to incomplete depolarization produced by the current supplied with the micropipette.

The endoneurium cell and the Schwann cell potential differences described in this work must not be confused either (*a*) with the monophasic action potentials (in many cases without measurable resting potential) observed by Tasaki (17) in myelinated frog sciatic fibers, which he attributed to a thin myelin film covering the electrode tip; or (*b*) with the stepwise resting and action potentials in the unmyelinated giant axon of the lobster, observed by Tobias and Bryant (18), which they considered to be due either to an incomplete entry in the axon of a bevelled microelectrode or to injury around the impalement site. The stepwise resting and action potentials described by Tobias and Bryant were sometimes observed by us in the squid nerve when three or more penetrations were performed through the same impalement site. These potentials probably result from the leakage of current around the micropipette. In these cases, when a depolarizing current was supplied inside the axon to diminish the potentials of the axon, a simultaneous and proportional variation of the stepwise resting and action potentials was produced. Thus, the interpretations of Tobias and Bryant as to the origin of the stepwise potentials appear to be correct.

The experiments reported in this section permit us to propose (*a*) that the endoneurium cell and the Schwann cell potential differences, studied in sections II and III, are electrically independent from that of the axon; and (*b*) that the well known action potentials which characterize the nerve fiber during impulse propagation occur across the axon plasma membrane, the axolemma. Thus, the axolemma appears to be the excitable membrane.

Our thanks are due to Dr. Guillermo Whittembury, Dr. Francisco Herrera, Dr. Lionel Warren, and Dr. Marcel Roche for reading the manuscript. We are indebted to Miss Gunilla Nalsen, Mr. José Mora, and Mr. José Bousquet for their technical assistance.
Received for publication, October 1, 1962.

BIBLIOGRAPHY

1. SCHMITT, F. O., *in* Metabolism of the Nervous System, (D. Richter, editor), New York, Pergamon Press Inc., 1957, 35.
2. SCHMITT, F. O., and GESCHWIND, N., *Progr. Biophysics and Biophysic. Chem.*, 1957, **8**, 166.
3. SJÖSTRAND, F., *in* Modern Scientific Aspects of Neurology, (J. N. Cumings, editor), London, Edward Arnold Ltd., 1960, 188.
4. FRANKENHAEUSER, B., and HODGKIN, A. L., *J. Physiol.*, 1956, **131**, 341.

5. VILLEGAS, G. M., and VILLEGAS, R., *J. Ultrastructure Research*, 1960, **3,** 362.
6. VILLEGAS, R., and VILLEGAS, G. M., *J. Gen. Physiol.*, 1960, **43,** No. 5, suppl., 73.
7. VILLEGAS, R., and BARNOLA, F. V., *J. Gen. Physiol.*, 1961, **44,** 963.
8. VILLEGAS, R., CAPUTO, C., and VILLEGAS, L., *J. Gen. Physiol.*, 1962, **46,** 245.
9. VILLEGAS, R., GIMÉNEZ, M., and VILLEGAS, L., *Biochim. et Biophysica Acta*, 1962, **62,** 610.
10. GEREN, B. B., and SCHMITT, F. O., *Proc. Nat. Acad. Sc.*, 1954, **40,** 863.
11. HODGKIN, A. L., and KATZ, B., *J. Physiol.*, 1949, **108,** 37.
12. LING, G., and GERARD, R. W., *J. Cell. and Comp. Physiol.*, 1949, **34,** 383.
13. ALEXANDER, J. T., and NASTUK, W. L., *Rev. Scient. Instr.*, 1953, **24,** 528.
14. VILLEGAS, L., *Biochim. et Biophysica Acta*, 1962, **64,** 359.
15. MITARAI, G., *J. Gen. Physiol.*, 1960, **43,** No. 6, suppl., 95.
16. WHITTEMBURY, G., *Am. J. Physiol.*, 1963, **204,** 401.
17. TASAKI, I., *Japan. J. Physiol.*, 1952, **3,** 73.
18. TOBIAS, J. M., and BRYANT, S. H., *J. Cell. and Comp. Physiol.*, 1955, **46,** 163.